

# Propagation of an electromagnetic wave in an absorbing anisotropic medium and infrared transmission of liquid crystals: Comparison with experiments

B. K. P. Scaife,<sup>1</sup> A. A. Sigarev,<sup>1,\*</sup> J. K. Vij,<sup>1,†</sup> and J. W. Goodby<sup>2</sup>

<sup>1</sup>*Department of Electronic and Electrical Engineering, Trinity College, University of Dublin, Dublin 2, Ireland*

<sup>2</sup>*Department of Chemistry, University of York, York YO10 5DD, United Kingdom*

(Received 25 May 2009; published 31 August 2009)

The theory of the absorbance of a semi-infinite medium characterized by a second-rank dielectric tensor for the entire electromagnetic spectrum, as given by Scaife and Vij [J. Chem. Phys. **122**, 174901 (2005)], is extended to include molecules of prolate spheroidal shape with longitudinal and transverse polarizabilities and to cover the case of elliptically polarized incident radiation. The theory is applied to the infrared transmission experiments of biaxial liquid crystals. It is found that the formula for the dependence on frequency and on angle of polarization of the absorbance  $\mathbf{A}(\omega, \theta) = -\log_{10}[10^{A(\omega, 0)} \cos^2 \theta + 10^{-A(\omega, \pi/2)} \sin^2 \theta]$  is unaffected by the anisotropy of the molecules and by the elliptical polarization of the incident radiation. A small ( $\pm 5\%$ ) discrepancy between theory and experiment has been found for bands with high absorbances. It is found that this discrepancy does not depend on birefringence of the sample but may depend on the precise method of absorbance measurement and on effects at the surface of the cell containing the liquid crystal under test.

DOI: [10.1103/PhysRevE.80.021704](https://doi.org/10.1103/PhysRevE.80.021704)

PACS number(s): 61.30.Gd, 42.70.Df, 77.84.Nh

## I. INTRODUCTION

In our previous paper [1], we developed the theory of the propagation of an electromagnetic homogeneous plane wave in a semi-infinite, optically anisotropic, and absorbing medium. A homogeneous wave is defined as one in which the planes of constant amplitude and of phase are parallel to each other. From first principles, we derived an equation for the infrared (IR) absorbance at a given frequency as a function of the angle of polarization  $\theta$  for normal incidence of an IR beam incident on a cell containing a ferroelectric liquid-crystalline sample between its windows. We also derived formulas for the various order parameters of a distribution function in terms of the electrical susceptibilities along different axes. The liquid-crystalline material is aligned in a planar configuration, where the molecules are aligned to lie along the surface of the windows and are confined within the windows of the cell. In the derivation, we considered the elements of the dielectric tensor to be complex and frequency dependent but the dependence of the wave vector on frequency was neglected. This was justified in view of the fact that the smectic layer thickness ( $\sim 3$  nm) was much lower than the shortest wavelength of the IR beam  $\sim 3$   $\mu$ m. A more general treatment of the propagation of the electromagnetic wave in an infinite medium was given by Yuan *et al.* [2,3] in which they considered spatial dispersion, i.e., the permittivity was dependent on the wave vector, in addition to the frequency. When we applied the theory to our infrared experiment, we obtained the following formula:

$$\mathbf{A}(\omega, \theta) = -\log_{10}[10^{-A_{\parallel}(\omega)} \cos^2 \theta + 10^{-A_{\perp}(\omega)} \sin^2 \theta], \quad (1)$$

where  $A_{\parallel}(\omega)$  and  $A_{\perp}(\omega)$  are the absorbances parallel and normal to the polarizer  $A_{\parallel}(\omega) = \mathbf{A}(\omega, 0)$  and  $A_{\perp}(\omega) = \mathbf{A}(\omega, \pi/2)$ .

\*Permanent address: Moscow Institute of Physics and Technologies, Dolgoprudnij, Moscow 141700, Russia.

†Author to whom correspondence should be addressed; [jvij@tcd.ie](mailto:jvij@tcd.ie)

We have already shown [1] that this formula, which was first proposed empirically by Jang *et al.* [4], is independent of the birefringence of the material subjected to the IR beam and, in general, to the biaxiality of the material. An earlier attempt was made in deriving this formula based on the rotation of the plane of polarization of light by the anisotropies in the infrared absorbances by Kocot *et al.* [5]. Equation (1) has been extensively used in analyzing IR data and in finding the orientational distribution function of the transition moment and, in particular, that of the carbonyl bond close to the chiral center [4,6–11]. In deriving Eq. (1), we assumed that the sample axes coincided with the principal axes of the permittivity tensor. The existence of these principal axes follows from the symmetry of the permittivity tensor, that is,

$$\varepsilon_{\alpha,\beta}(\omega) = \varepsilon_{\beta,\alpha}(\omega), \quad (2)$$

where the suffixes  $\alpha$  and  $\beta$  can take the values 1, 2, or 3. In view of the symmetry condition in Eq. (2), it is always possible to choose a set of coordinate axes so that the permittivity tensor becomes diagonal.

## II. MICROSCOPIC CONSIDERATIONS

In the analysis that we carried out, we assumed that the medium consisted of long rodlike molecules having an axial polarizability only. However, if the polarizability or—more specifically—the moment of a vibrational bond of the molecule lies at an angle to the major axis of the molecule, then this case may not be covered in such an analysis. We therefore extend the analysis in this paper to include the treatment of molecules as prolate spheroids having both axial  $a_{\parallel}$  and transverse  $a_{\perp}$  polarizabilities measured with reference to the principal axes. This means that if in an actual system the polarizability were out of the plane to which the incident light is directed normally, then due to the symmetry of the rotation of the molecules this should not affect results of the calculations. If the angular coordinates of a molecule are  $\beta$ ,

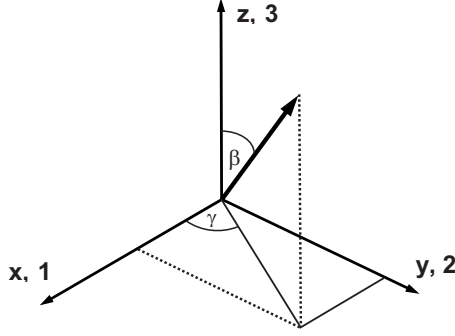


FIG. 1. The angular coordinates  $\beta$  and  $\gamma$  specify the orientation of a molecule with respect to the axes 1, 2, and 3 or  $x$ ,  $y$ , and  $z$  axes.

$\gamma$  as in Fig. 1. The orientational distribution function  $\rho(\beta, \gamma)$  can be taken to be [12]

$$4\pi\rho(\beta, \gamma) = 1 + 3A \sin \beta \sin \gamma + 5BP_2(\cos \beta) + (15/4) \\ \times [C \sin 2\beta \cos \gamma + D \sin^2 \beta \cos 2\gamma \\ + E \sin 2\beta \sin \gamma + F \sin^2 \beta \sin 2\gamma]. \quad (3)$$

Here  $A$ ,  $B$ ,  $C$ ,  $D$ ,  $E$ , and  $F$  are the expansion coefficients and these serve as the order parameters with the maximum value of 1 in a completely ordered systems.  $B$  is the orientational order parameter known more commonly as the order parameter  $S$ . The simpler forms of the distribution function may contain only a few order parameters [13].

In this analysis we assume, as before, that the permittivity tensor is diagonal,

$$[\varepsilon_{\alpha\beta}(\omega)] = \begin{bmatrix} \varepsilon_1(\omega) & 0 & 0 \\ 0 & \varepsilon_2(\omega) & 0 \\ 0 & 0 & \varepsilon_3(\omega) \end{bmatrix},$$

where we use the abbreviations  $\varepsilon_{1,1}(\omega) = \varepsilon_1(\omega)$ ,  $\varepsilon_{2,2}(\omega) = \varepsilon_2(\omega)$ , and  $\varepsilon_{3,3}(\omega) = \varepsilon_3(\omega)$ .

By extending Eqs. (5.3a)–(5.3c) in our previous paper [1], we obtain the three polarization components  $p_1$ ,  $p_2$ , and  $p_3$  along the axes 1, 2, and 3, with angles with respect to the coordinates as shown in Fig. 1,

$$p_{1,1} = \chi_{1,1}\epsilon_0 e_1 \\ = \frac{N}{V} e_1 \{ \alpha_{\parallel} \langle \sin^2 \beta \cos^2 \gamma \rangle + \alpha_{\perp} \langle \cos^2 \beta \cos^2 \gamma + \sin^2 \gamma \rangle \} \\ = \frac{N}{V} e_1 \{ \alpha_{\parallel} \langle \sin^2 \beta \cos^2 \gamma \rangle + \alpha_{\perp} \langle 1 - \sin^2 \beta \cos^2 \gamma \rangle \}, \quad (4)$$

$$p_{2,1} = \chi_{2,1}\epsilon_0 e_1 \\ = \frac{N}{V} e_1 \{ \alpha_{\parallel} \langle \sin^2 \beta \sin \gamma \cos \gamma \rangle \\ + \alpha_{\perp} \langle \cos^2 \beta \sin \gamma \cos \gamma - \sin \gamma \cos \gamma \rangle \} \\ = \frac{N}{V} e_1 \{ \alpha_{\parallel} \langle \sin^2 \beta \sin \gamma \cos \gamma \rangle + \alpha_{\perp} \langle -\sin^2 \beta \sin \gamma \cos \gamma \rangle \}, \quad (5)$$

$$p_{3,1} = \chi_{3,1}\epsilon_0 e_1 \\ = \frac{N}{V} e_1 \{ \alpha_{\parallel} \langle \sin \beta \cos \beta \cos \gamma \rangle - \alpha_{\perp} \langle \sin \beta \cos \beta \cos \gamma \rangle \}, \quad (6)$$

$$p_{1,2} = \chi_{1,2}\epsilon_0 e_2 \\ = \frac{N}{V} e_2 \{ \alpha_{\parallel} \langle \sin^2 \beta \sin \gamma \cos \gamma \rangle \\ + \alpha_{\perp} \langle \cos^2 \beta \sin \gamma \cos \gamma - \sin \gamma \cos \gamma \rangle \} \\ = \frac{N}{V} e_2 \{ \alpha_{\parallel} \langle \sin^2 \beta \sin \gamma \cos \gamma \rangle \\ + \alpha_{\perp} \langle -\sin^2 \beta \sin \gamma \cos \gamma \rangle \}, \quad (7)$$

$$p_{2,2} = \chi_{2,2}\epsilon_0 e_2 \\ = \frac{N}{V} e_2 \{ \alpha_{\parallel} \langle \sin^2 \beta \sin^2 \gamma \rangle + \alpha_{\perp} \langle \cos^2 \beta \sin^2 \gamma + \cos^2 \gamma \rangle \} \\ = \frac{N}{V} e_2 \{ \alpha_{\parallel} \langle \sin^2 \beta \sin^2 \gamma \rangle + \alpha_{\perp} \langle 1 - \sin^2 \beta \sin^2 \gamma \rangle \}, \quad (8)$$

$$p_{3,2} = \chi_{3,2}\epsilon_0 e_2 \\ = \frac{N}{V} e_2 \{ \alpha_{\parallel} \langle \sin \beta \cos \beta \sin \gamma \rangle + \alpha_{\perp} \langle -\sin \beta \cos \beta \sin \gamma \rangle \}, \quad (9)$$

$$p_{1,3} = \chi_{1,3}\epsilon_0 e_3 \\ = \frac{N}{V} e_1 \{ \alpha_{\parallel} \langle \sin \beta \cos \beta \cos \gamma \rangle - \alpha_{\perp} \langle \sin \beta \cos \beta \cos \gamma \rangle \}, \quad (10)$$

$$p_{2,3} = \chi_{2,3}\epsilon_0 e_3 \\ = \frac{N}{V} e_2 \{ \alpha_{\parallel} \langle \sin \beta \cos \beta \sin \gamma \rangle - \alpha_{\perp} \langle \sin \beta \cos \beta \sin \gamma \rangle \}, \quad (11)$$

$$p_{3,3} = \chi_{3,3}\epsilon_0 e_3 = \frac{N}{V} e_3 \{ \alpha_{\parallel} \langle \cos^2 \beta \rangle + \alpha_{\perp} \langle \sin^2 \beta \rangle \}. \quad (12)$$

With Eqs. (A1)–(A6) of [1], we find that

$$p_{1,1} = \chi_{1,1}\epsilon_0 e_1 \\ = \frac{N}{V} e_1 \left\{ \frac{\alpha_{\parallel}}{3} \left[ 1 - B + \frac{3D}{2} \right] + \frac{\alpha_{\perp}}{3} \left[ 2 + B - \frac{3D}{2} \right] \right\}, \quad (13)$$

$$p_{2,1} = \chi_{2,1}\epsilon_0 e_1 = \frac{N}{V} e_1 \left\{ \alpha_{\parallel} \frac{F}{2} - \alpha_{\perp} \frac{F}{2} \right\}, \quad (14)$$

$$p_{3,1} = \chi_{3,1}\epsilon_0 e_1 = \frac{N}{V} e_1 \left\{ \alpha_{\parallel} \frac{C}{2} - \alpha_{\perp} \frac{C}{2} \right\}, \quad (15)$$

$$p_{1,2} = \chi_{1,2} \epsilon_0 e_2 = \frac{N}{V} e_2 \left\{ \alpha_{\parallel} \frac{F}{2} - \alpha_{\perp} \frac{F}{2} \right\}, \quad (16)$$

$$\begin{aligned} p_{2,2} &= \chi_{2,2} \epsilon_0 e_2 \\ &= \frac{N}{V} e_2 \left\{ \frac{\alpha_{\parallel}}{3} \left[ 1 - B - \frac{3D}{2} \right] + \frac{\alpha_{\perp}}{3} \left[ 2 + B + \frac{3D}{2} \right] \right\}, \end{aligned} \quad (17)$$

$$p_{3,2} = \chi_{3,2} \epsilon_0 e_2 = \frac{N}{V} e_2 \left\{ \alpha_{\parallel} \frac{E}{2} - \alpha_{\perp} \frac{E}{2} \right\}, \quad (18)$$

$$p_{1,3} = \chi_{1,3} \epsilon_0 e_3 = \frac{N}{V} e_3 \left\{ \alpha_{\parallel} \frac{C}{2} - \alpha_{\perp} \frac{C}{2} \right\}, \quad (19)$$

$$p_{2,3} = \chi_{2,3} \epsilon_0 e_3 = \frac{N}{V} e_3 \left\{ \alpha_{\parallel} \frac{E}{2} - \alpha_{\perp} \frac{E}{2} \right\}, \quad (20)$$

$$p_{3,3} = \chi_{3,3} \epsilon_0 e_3 = \frac{N}{V} e_3 \left\{ \frac{\alpha_{\parallel}}{3} [1 + 2B] + \frac{2\alpha_{\perp}}{3} [1 - B] \right\}. \quad (21)$$

Therefore, the components of susceptibility  $\chi_1$ ,  $\chi_2$ , and  $\chi_3$ , along the axes 1, 2, and 3 are

$$\chi_{1,1} = \frac{N}{\epsilon_0 V} \left\{ \frac{(\alpha_{\parallel} + 2\alpha_{\perp})}{3} + \frac{(\alpha_{\parallel} - \alpha_{\perp})}{3} \left( -B + \frac{3D}{2} \right) \right\}, \quad (22)$$

$$\chi_{2,1} = \frac{N}{\epsilon_0 V} \left\{ (\alpha_{\parallel} - \alpha_{\perp}) \frac{F}{2} \right\}, \quad (23)$$

$$\chi_{3,1} = \frac{N}{\epsilon_0 V} \left\{ (\alpha_{\parallel} - \alpha_{\perp}) \frac{C}{2} \right\}, \quad (24)$$

$$\chi_{1,2} = \frac{N}{\epsilon_0 V} \left\{ (\alpha_{\parallel} - \alpha_{\perp}) \frac{F}{2} \right\}, \quad (25)$$

$$\chi_{2,2} = \frac{N}{\epsilon_0 V} \left\{ \frac{(\alpha_{\parallel} + 2\alpha_{\perp})}{3} + \frac{(\alpha_{\parallel} - \alpha_{\perp})}{3} \left( -B - \frac{3D}{2} \right) \right\}, \quad (26)$$

$$\chi_{3,2} = \frac{N}{\epsilon_0 V} \left\{ (\alpha_{\parallel} - \alpha_{\perp}) \frac{E}{2} \right\}, \quad (27)$$

$$\chi_{1,3} = \frac{N}{\epsilon_0 V} \left\{ (\alpha_{\parallel} - \alpha_{\perp}) \frac{C}{2} \right\}, \quad (28)$$

$$\chi_{2,3} = \frac{N}{\epsilon_0 V} \left\{ (\alpha_{\parallel} - \alpha_{\perp}) \frac{E}{2} \right\}, \quad (29)$$

$$\chi_{3,3} = \frac{N}{\epsilon_0 V} \left\{ \frac{(\alpha_{\parallel} + 2\alpha_{\perp})}{3} + \frac{(\alpha_{\parallel} - \alpha_{\perp})}{3} 2B \right\}. \quad (30)$$

Equations (22)–(30) can be expressed in terms of the following matrix equation:

$$\frac{\epsilon_0 V}{N} \begin{bmatrix} \chi_{1,1} & \chi_{1,2} & \chi_{1,3} \\ \chi_{2,1} & \chi_{2,2} & \chi_{2,3} \\ \chi_{3,1} & \chi_{3,2} & \chi_{3,3} \end{bmatrix} = \begin{bmatrix} \bar{\alpha} + \Delta \left( -\frac{B}{3} + \frac{D}{2} \right) & \Delta \frac{F}{2} & \Delta \frac{C}{2} \\ \Delta \frac{F}{2} & \bar{\alpha} + \Delta \left( -\frac{B}{3} - \frac{D}{2} \right) & \Delta \frac{E}{2} \\ \Delta \frac{C}{2} & \Delta \frac{E}{2} & \bar{\alpha} + \Delta \frac{2B}{3} \end{bmatrix}, \quad (31)$$

where  $\bar{\alpha} \equiv \left( \frac{\alpha_{\parallel} + 2\alpha_{\perp}}{3} \right)$  and  $\Delta \equiv (\alpha_{\parallel} - \alpha_{\perp})$ .

Clearly we find that  $\chi_{i,j} = \chi_{j,i}$ . This is of the same form as matrix (5.12) of our previous paper [1], except that the permittivity in different directions is related explicitly with the anisotropy in the polarizability  $\Delta$  and the averaged polarizability  $\bar{\alpha}$ . The matrix (31) can be used to relate the various order parameters of the distribution function to the averaged polarizability, the birefringence, and the components of the electrical susceptibilities along different axes. By using Eqs. (22) and (26), the order parameters  $B$  and  $D$  can be found from the susceptibilities by the following equations:

$$B = \frac{3}{\Delta} \left[ \bar{\alpha} - \frac{\epsilon_0 V}{2N} (\chi_{1,1} + \chi_{2,2}) \right], \quad (32)$$

$$D = \frac{\epsilon_0 V}{N\Delta} (\chi_{1,1} - \chi_{2,2}). \quad (33)$$

The order parameters  $C$ ,  $E$ , and  $F$  can similarly be found by using Eqs. (27)–(29).

### III. POYNTING VECTOR AND TRANSMISSION THROUGH THE IR CELL

#### Case of elliptically polarized light

In our previous analysis, we considered the incident IR beam to be plane polarized, which makes an angle  $\theta$  with the  $z$  axis. Now we extend this analysis to include elliptically

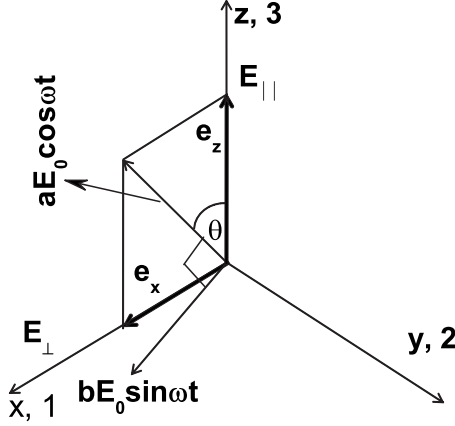


FIG. 2. The elliptical polarized light incident along the axis  $y$  or 2. The component  $aE_0 \cos \omega t$  makes an angle  $\theta$  with respect to the axis  $z$  or 3.

polarized light as shown in Fig. 2 with two orthogonal components  $aE_0 \cos \omega t$  and  $bE_0 \sin \omega t$  lying in the  $x$ - $z$  plane. The component  $aE_0 \cos \omega t$  makes an angle  $\theta$  with the  $z$  axis, so that

$$e_z = aE_0 \cos \omega t \cos \theta - bE_0 \sin \omega t \sin \theta, \quad (34)$$

$$e_x = aE_0 \cos \omega t \sin \theta + bE_0 \sin \omega t \cos \theta, \quad (35)$$

and

$$e_z = E_0 \operatorname{Re}[a \cos \theta + ib \sin \theta] \varepsilon^{i\omega t}, \quad (36)$$

$$e_x = E_0 \operatorname{Re}[a \cos \theta - ib \sin \theta] \varepsilon^{i\omega t}. \quad (37)$$

In place of Eq. (3.4a) of our previous analysis [1], we would have the total electric field vector within the sample

$$\begin{aligned} \vec{e}(\vec{r}, t) = \operatorname{Re}\{ & \vec{i}_1 E_{in} [a \cos \theta - ib \sin \theta] F_{\perp, E} C_{\perp, E} \varepsilon^{i(\omega t - k_{\perp} y)} \\ & + \vec{i}_3 E_{in} [a \cos \theta + ib \sin \theta] F_{\parallel, E} C_{\parallel, E} \varepsilon^{i(\omega t - k_{\parallel} y)} \}, \end{aligned} \quad (38)$$

and in place of Eq. (3.4b) [1] we have the magnetizing force vector in the sample

$$\begin{aligned} \vec{h}(\vec{r}, t) = \frac{1}{\omega \mu_0} \operatorname{Re} \varepsilon^{i\omega t} E_{in} \{ & -\vec{i}_3 (a \sin \theta - ib \cos \theta) k_{\perp}(\omega) \\ & \times F_{\perp, E}(\omega) C_{\perp, H}(\omega) \varepsilon^{-ik_{\perp} y} \} + \{ -\vec{i}_1 (a \cos \theta \\ & + ib \sin \theta) k_{\parallel}(\omega) F_{\parallel, E}(\omega) C_{\parallel, H}(\omega) \varepsilon^{-ik_{\parallel} y} \}. \end{aligned} \quad (39)$$

If we continue the procedure of calculations as in [1], we will find the Poynting vector in the cell normal to the plane of the cell windows to be

$$\begin{aligned} \vec{S}(y) = \vec{i}_2 \frac{2}{\omega \mu_0} \operatorname{Re} |E_0(\omega)|^2 \{ & \varepsilon^{-2k_{\perp} y} (a^2 \sin^2 \theta + b^2 \cos^2 \theta) \\ & \times |F_{\perp, E}(\omega)|^2 k_{\perp}^*(\omega) C_{\perp, y}(\omega, y) C_{\perp, H}^*(\omega) \\ & + \varepsilon^{-2k_{\parallel} y} (a^2 \cos^2 \theta + b^2 \sin^2 \theta) |F_{\parallel, E}(\omega)|^2 k_{\parallel}^*(\omega) C_{\parallel, y} C_{\parallel, H}^* \}, \end{aligned} \quad (40)$$

in place of Eq. 3.7 of [1].

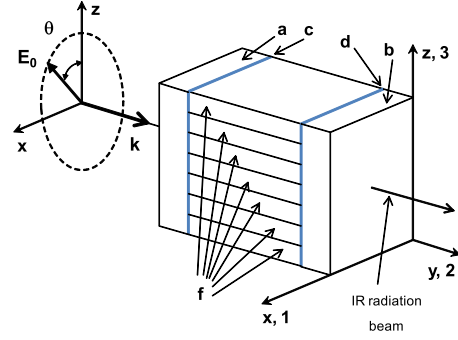


FIG. 3. (Color online) The schematic experimental arrangement for IR spectroscopy. The radiation of wave vector  $\mathbf{k}$  propagates along the  $y$  or 2 axis. The sample lies in between two [(a) and (b)]  $\text{CaF}_2$  windows, each with an indium tin oxide electrode treated with a polymer [(c) and (d)]. The smectic layers (f) lie in the  $x, y$  plane. The electric vector  $\mathbf{E}_0$  of the polarized radiation is perpendicular to  $\mathbf{k}$  and makes an angle  $\theta$  with the  $z$  axis, which is taken as the principal optical axis.

We apply this analysis to an IR cell. The intensity of the IR beam is somewhat attenuated by the windows of the cell, we work out the mean power density emerging from the cell  $P_{out}(\omega, \theta)$ . Recalling the definition of the transmission of the cell as the ratio of the incident power density to that exiting the cell, we find

$$\begin{aligned} T_{cell}(\omega, \theta) &= \frac{P_{out}(\omega, \theta)}{P_{in}(\omega, \theta)} [\Lambda_{\parallel} (a^2 \cos^2 \theta + b^2 \sin^2 \theta) \\ &+ \Lambda_{\perp} (a^2 \sin^2 \theta + b^2 \cos^2 \theta)] \\ &= \frac{P_{out}(\omega, \theta)}{P_{in}(\omega, \theta)} [(\Lambda_{\parallel} a^2 + \Lambda_{\perp} b^2) \\ &\times \cos^2 \theta (\Lambda_{\parallel} b^2 + \Lambda_{\perp} a^2) \sin^2 \theta], \end{aligned} \quad (41)$$

which has the same form as the original Eq. (3.14) of our analysis [1]. If  $a$  and  $b$  were independent of  $\theta$ , we arrive at a result similar to Eq. (1).

#### IV. EXPERIMENT

We show the experimental data on the absorbance of three bands as a function of the angle of polarization of the incident IR beam for a liquid-crystalline material. The molecules of the material are aligned homogeneously on the substrates, the surfaces of the latter were rubbed so as to have a planar alignment of the molecules along a specific direction. This was achieved by assembling the substrates that are parallel rubbed to form a cell with a cell spacing of  $6 \mu\text{m}$  thickness. Fields of different constant strengths were applied across the cell. The geometrical arrangement of the experimental setup is given in Fig. 3. The compound with the chemical name (*S*)-4-(1-methylheptyloxycarbonylphenyl)-4'-[6-(3,4,4,4-tetrafluoromethylbutylcarbonyloxy)hexyloxy] biphenyl-4-carboxylate and an acronym of MHPHFHBOC (laboratory name AH43), (chemical formula given in Ref. [11], Fig. 1) was synthesized with a partly fluorinated achiral tail in the laboratory of Goodby. The phase sequence of the compound

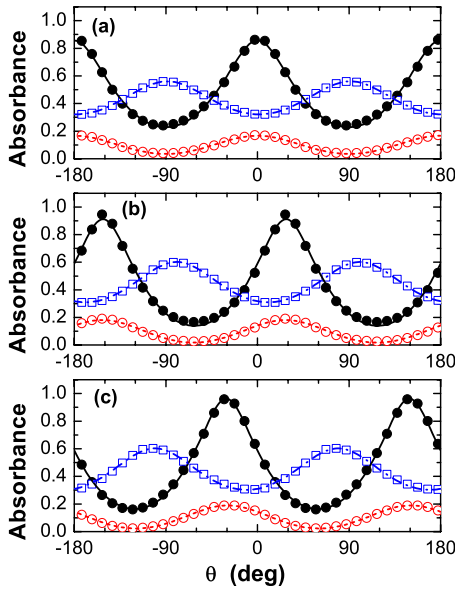


FIG. 4. (Color online) The absorbance  $A(\theta)$  as a function of the polarization angle  $\theta$  for the phenyl bands at  $1525\text{ cm}^{-1}$  ( $\circ$ ) and  $1603\text{ cm}^{-1}$  ( $\bullet$ ) and for the carbonyl band at  $1715\text{ cm}^{-1}$  ( $\square$ ) for MHPHFHHOBB in a  $6\text{ }\mu\text{m}$  cell at a temperature of  $122\text{ }^\circ\text{C}$ . Voltages applied across the cell are (a)  $V_{DC}=0\text{ V}$ , (b)  $V_{DC}=160\text{ V}$ , and (c)  $V_{DC}=-160\text{ V}$ . The fitted curves shown by the continuous and dotted lines are obtained using Eq. (1). In color online: red represents the band at  $1525\text{ cm}^{-1}$ , blue represents the band at  $1715\text{ cm}^{-1}$ , and black represents the band at  $1603\text{ cm}^{-1}$ .

obtained on cooling using polarized optical microscopy and IR spectroscopy on a homogeneously aligned sample was Iso  $125.3\text{ }^\circ\text{C}$   $\text{SmA}^*$   $120.2\text{ }^\circ\text{C}$   $\text{SmC}^*$   $115\text{ }^\circ\text{C}$   $\text{SmC}_A^*$   $57.5\text{ }^\circ\text{C}$  crystalline using polarized optical microscopy and IR spectroscopy on a homogeneously aligned sample of the compound in a cell of  $6\text{ }\mu\text{m}$  thickness. For a temperature of  $122\text{ }^\circ\text{C}$  in the  $\text{SmA}^*$  phase at zero field, the results of absorbance for the in-plane C-C stretching vibration bands at  $1525\text{ cm}^{-1}$  and  $1603\text{ cm}^{-1}$  and the carbonyl band near the chiral center of  $1715\text{ cm}^{-1}$  are shown in Fig. 4. The fitting of the data to Eq. (1) is shown by continuous, dashed, and dotted lines. The in-plane stretching vibration at  $1603\text{ cm}^{-1}$  band has higher absorbances than the other two bands. We find that the fitting of the data to the highest absorbance band is poorer than either of the other two bands. The results for temperatures in the  $\text{SmC}^*$  and  $\text{SmC}_A^*$  (phases in the zero-field condition) are given in Figs. 5 and 6.

When the external voltage is applied, the material is in a different state than in the absence of the field. The fitting of the experimental results to Eq. (1) is again shown by lines that join the data points. The overall conclusion is that Eq. (1) fits the data reasonably well except at the two extremities of the maximum and the minimum absorbances. This is clarified in Fig. 7, where the data of Fig. 5 are magnified both for the strongest and the weakest absorbance bands at a temperature in the  $\text{SmA}^*$  (again only in the absence of the external field) for both positive and negative voltages. The discrepancy  $A_{exp}(\theta)-A_{fit}(\theta)$  as a function of the angle of polarization  $\theta$  for the data presented in Fig. 7 (as per one example) for the two bands are shown in Fig. 8. From Fig. 8, we find that the

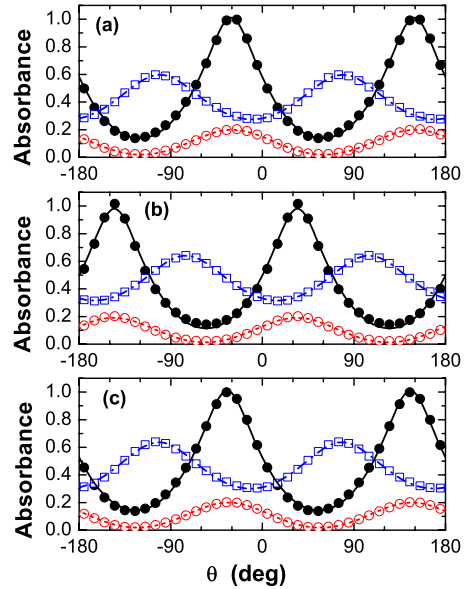


FIG. 5. (Color online) The absorbance  $A(\theta)$  as a function of the polarization angle  $\theta$  for the phenyl bands at  $1525\text{ cm}^{-1}$  ( $\circ$ ) and  $1603\text{ cm}^{-1}$  ( $\bullet$ ) and for the carbonyl band at  $1715\text{ cm}^{-1}$  ( $\square$ ) for MHPHFHHOBB in a  $6\text{ }\mu\text{m}$  cell at a temperature of  $118\text{ }^\circ\text{C}$  in  $\text{SmC}^*$  at zero field across the cell. Voltages applied across the cell are (a)  $V_{DC}=0\text{ V}$ , (b)  $V_{DC}=40\text{ V}$ , and (c)  $V_{DC}=-40\text{ V}$ . The fitted curves to Eq. (1) are shown by the continuous and dotted lines. In color online: red represents the band at  $1525\text{ cm}^{-1}$ , blue represents the band at  $1715\text{ cm}^{-1}$ , and black represents the band at  $1603\text{ cm}^{-1}$ .

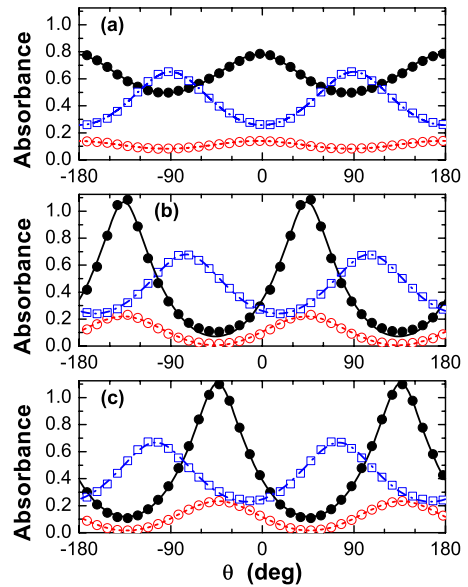


FIG. 6. (Color online) The absorbance  $A(\theta)$  as a function of the polarization angle  $\theta$  for the phenyl bands at  $1525\text{ cm}^{-1}$  ( $\circ$ ) and  $1603\text{ cm}^{-1}$  ( $\bullet$ ) and for the carbonyl band at  $1715\text{ cm}^{-1}$  ( $\square$ ) for MHPHFHHOBB in a  $6\text{ }\mu\text{m}$  cell at a temperature of  $65\text{ }^\circ\text{C}$  in the  $\text{SmC}_A^*$  at zero field across the cell. Voltages applied across the cell are (a)  $V_{DC}=0\text{ V}$ , (b)  $V_{DC}=40\text{ V}$ , and (c)  $V_{DC}=-40\text{ V}$ . Fitted curves shown by continuous and dotted lines are obtained using Eq. (1). In color online: red represents the band at  $1525\text{ cm}^{-1}$ , blue represents the band at  $1715\text{ cm}^{-1}$ , and black represents the band at  $1603\text{ cm}^{-1}$ .

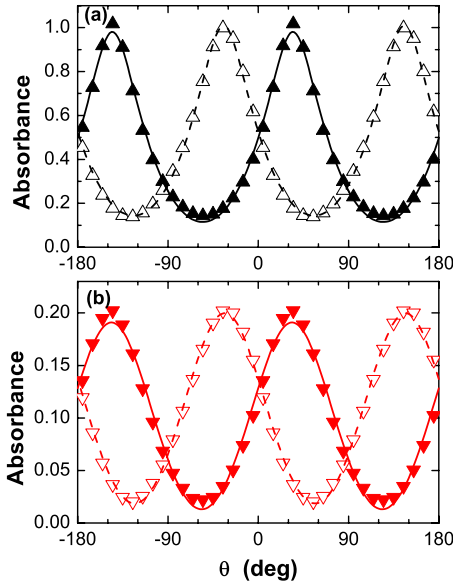


FIG. 7. (Color online) Fitting to Eq. (1) is shown for the data in Fig. 5 for the bands (a)  $1603\text{ cm}^{-1}$ ,  $+40\text{ V}$  ( $\blacktriangle$ );  $1603\text{ cm}^{-1}$ ,  $-40\text{ V}$  ( $\triangle$ ); (b)  $1525\text{ cm}^{-1}$ ,  $+40\text{ V}$  ( $\blacktriangledown$ ); and  $1525\text{ cm}^{-1}$ ,  $-40\text{ V}$  ( $\triangledown$ ) at a temperature of  $118\text{ }^\circ\text{C}$ . The experimental data points are marked, whereas the fitting to Eq. (1) is given by the continuous and dotted lines. In color online: red represents the band at  $1525\text{ cm}^{-1}$ , and black the band at  $1603\text{ cm}^{-1}$ .

maximum discrepancy occurs during the two extremities maximum and minimum absorbances. Nevertheless, the maximum error in the fitting of the data to the experiment is  $\pm 5\%$ . The possible reasons for the discrepancy are given in the next section.

## V. DISCUSSION

First we find that the formula (1) is independent of the birefringence also for the two cases considered in this paper. Jang *et al.* [14] stated that Eq. (1) is exact only for zero birefringence and they justify it on the basis that it is almost zero in the given experiments particularly “when the eigenmodes of a dichroic medium are linearly polarized along the directions of maximum and minimum absorbances. For the vibrations polarized nearly along the optic axis of the real part of the dielectric constant, the birefringence can be ignored in a few  $\mu\text{m}$  thick samples.” This means that when the absorbance is maximum or minimum, the real part of the permittivity along the two axes is the same. In our view, this is very unlikely to be the case. For the case of a planarly aligned cell as is the case here, even if the light were polarized parallel to the optical axis of maximum permittivity, the biaxiality would play a role. In the given experiment, however, the angle of polarization is varied and the absorbance is studied as a function of this angle. Consequently, the birefringence experienced by the IR beam is not zero and is dependent on the angle of polarization. From the examination of Fig. 8, we find that the fitting has a maximum error of  $\pm 5\%$  in absorbance close to the extremities of the absorbance. The error in between the theory and the experiments

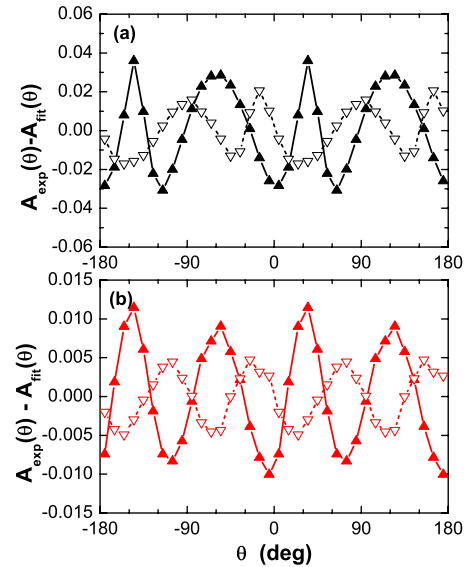


FIG. 8. (Color online) The deviations  $[A_{exp}(\theta_i) - A_{fit}(\theta_i)]$  of the experimental data in Fig. 5 for the bands at (a)  $1603\text{ cm}^{-1}$ ,  $+40\text{ V}$  ( $\blacktriangleright$ );  $1603\text{ cm}^{-1}$ ,  $-40\text{ V}$  ( $\triangleright$ );  $1525\text{ cm}^{-1}$ ,  $+40\text{ V}$  ( $\blacktriangleleft$ ); and (b) at the band  $1525\text{ cm}^{-1}$ ,  $-40\text{ V}$  ( $\triangleleft$ ) from the fitted equation as a function of the polarization angle. This illustration corresponds to the data shown in Fig. 7. In color online: red represents the band at  $1525\text{ cm}^{-1}$ , and black represents the band at  $1603\text{ cm}^{-1}$ .

is somewhat higher when voltage applied is of positive polarity as compared to when the polarity is reversed. In any case, the percentage error based on the results seems to be independent of the strength of the absorbance. One can reasonably expect that the IR birefringence is higher for the band with a higher absorbance. The errors in fitting are thus found to be independent of the magnitude of birefringence. Thus, the latter playing any role in the discrepancy between the theory as given by Eq. (1) and the experimental data is ruled out. One of the reasons for the small discrepancy may possibly arise from the manner in which the absorbance is calculated. The maximum absorbance of the IR band is calculated from the definition of the absorbance,

$$A(\omega, \theta) \equiv -\log_{10} T_{cell}(\omega, \theta), \quad (42)$$

where

$$T_{cell}(\omega, \theta) \equiv \frac{I_{out}(\omega, \theta)}{I_{in}(\omega, \theta)}. \quad (43)$$

For higher absorbances, one may obtain a considerable error in calculating the exact value of the absorbance for the reason that the transmission through the cell  $T_{cell}(\omega, \theta)$  is low. The error in the logarithmic value of the transmission will increase further. This could in principle alter the fitting and make it bad for higher absorbance bands in particular.

Another likely source of the error is possibly the effect due to the surfaces. The surface treatment of substrates of the cell is used to align the liquid-crystalline molecules and the relative alignment of the molecules is likely to vary in the

bulk with the distance from the substrate. It seems very likely that the alignment through out the bulk of the cell is not as uniform as on the surfaces.

A comparison of the theory with the experiments shows that IR birefringence as stated above plays no role in Eq. (1) for the absorbance as a function of the polarization angle of the incident IR beam. This formula (1) is also independent of whether the molecules of the liquid-crystalline system are needle shaped or ellipsoidal or whether the incident light is plane or circularly polarized.

The underlying assumption that the principal axes of the system coincide with the axes of the permittivity tensor may strictly be not valid for the liquid-crystalline systems and this problem needs to be explored further.

#### ACKNOWLEDGMENTS

The authors thank Uttam Manna for organizing the figures. The work was funded partly by the SFI (Grant No. 02/W/I02) and RFP ENE Grant No. 06/0039. The IR spectroscopic measurements were made using the sample synthesized in the laboratory of Professor J. W. Goodby under the European SAMPA research project (2002–2006).

#### APPENDIX

A few typographic errors in our previous paper [1] corrected are being listed here. Equation (5.3c) should be read as

$$p_{3,1} = \chi_{3,1}\epsilon_0 e_1 = \frac{N}{V} \langle \alpha_s e_1 \cos \gamma \cos \beta \sin \beta \rangle = (\epsilon_{3,1} - 1)\epsilon_0 e_1. \quad (\text{A1})$$

Equation (5.7a) should be read as

$$p_{1,3} = \chi_{1,3}\epsilon_0 e_3 = \frac{N}{V} \langle \alpha_s e_3 \cos \gamma \sin \beta \cos \beta \rangle = (\epsilon_{1,3} - 1)\epsilon_0 e_3. \quad (\text{A2})$$

Equation (5.7b) should be read as

$$p_{2,3} = \chi_{2,3}\epsilon_0 e_3 = \frac{N}{V} \langle \alpha_s e_3 \sin \gamma \sin \beta \cos \beta \rangle = (\epsilon_{2,3} - 1)\epsilon_0 e_3. \quad (\text{A3})$$

Equation (5.7c) should be read as

$$p_{3,3} = \chi_{3,3}\epsilon_0 e_3 = \frac{N}{V} \langle \alpha_s e_3 \cos^2 \beta \rangle = (\epsilon_3 - 1)\epsilon_0 e_3. \quad (\text{A4})$$

- 
- [1] B. K. P. Scaife and J. K. Vij, *J. Chem. Phys.* **122**, 174901 (2005).
- [2] H. Yuan, E. Weinan, and P. Palffy-Muhoray, *Phys. Rev. E* **61**, 3264 (2000).
- [3] H. Yuan, W. E. Palffy-Mohoray, and P. Palffy-Muhoray, *Mol. Cryst. Liq. Cryst.* **358**, 311 (2001).
- [4] W. G. Jang, C. S. Park, J. E. McLennan, K. H. Kim, and N. A. Clark, *Ferroelectrics* **180**, 213 (1996).
- [5] A. Kocot, R. Wrzalik, and J. K. Vij, *Liq. Cryst.* **21**, 147 (1996).
- [6] K. H. Kim, K. Ishikawa, H. Takezoe, and A. Fukuda, *Phys. Rev. E* **51**, 2166 (1995).
- [7] A. Kocot, R. Wrzalik, B. Orgasinska, T. Perova, J. K. Vij, and H. T. Nguyen, *Phys. Rev. E* **59**, 551 (1999).
- [8] A. Kocot, J. K. Vij, and T. S. Perova, in *Adv. in Chem. Phys.*, edited by J. K. Vij, *Advances in Liquid Crystals* (Wiley, New York/Interscience, New York, 2000), Vol. 113, p. 203.
- [9] A. A. Sigarev, J. K. Vij, Yu. P. Panarin, and J. W. Goodby, *Phys. Rev. E* **62**, 2269 (2000).
- [10] A. A. Sigarev, J. K. Vij, R. A. Lewis, M. Hird, and J. W. Goodby, *Phys. Rev. E* **68**, 031707 (2003).
- [11] A. A. Sigarev, J. K. Vij, A. W. Hall, S. J. Cowling, and J. W. Goodby, *Phys. Rev. E* **76**, 051707 (2007).
- [12] M. Zgonik, M. Rey-Lafon, C. Destrade, C. Leon, and H. T. Nguyen, *J. Phys. (France)* **51**, 2015 (1990).
- [13] E. Hild, A. Kocot, J. K. Vij, and R. Zentel, *Liq. Cryst.* **16**, 783 (1994).
- [14] W. G. Jang, C. S. Park, and N. A. Clark, *Phys. Rev. E* **62**, 5154 (2000).